

We are IntechOpen, the world's leading publisher of Open Access books Built by scientists, for scientists

6,900

Open access books available

185,000

International authors and editors

200M

Downloads

Our authors are among the

154

Countries delivered to

TOP 1%

most cited scientists

12.2%

Contributors from top 500 universities



WEB OF SCIENCE™

Selection of our books indexed in the Book Citation Index
in Web of Science™ Core Collection (BKCI)

Interested in publishing with us?
Contact book.department@intechopen.com

Numbers displayed above are based on latest data collected.
For more information visit www.intechopen.com



Peculiarities of Electron Transfer in Chiral Linked Systems

*Aleksandra Ageeva, Ekaterina Khramtsova, Ilya Magin,
Nikolay Polyakov, Miguel Miranda and Tatyana Leshina*

Abstract

Electron transfer (ET) is one of the most universal reactions in chemistry and biology. Recent studies conducted on the examples of photoinduced ET (PET) in chiral linked systems (dyads) have shown several important features indicative for ET in chiral systems. The peculiarity of processes with PET in such systems is primarily the stereoselectivity; there is difference in ET rates and fluorescence quantum yields in dyad diastereomers. The next feature is the spin selectivity of back ET in the biradical-zwitterions (BZs) that are formed under the dyad diastereomer UV irradiation. This is the difference in the enhancement coefficients of chemically induced dynamic nuclear polarization (CIDNP) originated in BZs. The probable cause of this effect is the variation in the spin density values, resulting from difference in the spatial structure of BZ in (R,S)- and (S,S)-configurations. The latter, in turn, is due to the fact that these dyads react in the form of associates—dimers. The impact of dimerization on the effectiveness of ET in chiral systems is an example of the chiral catalysis. The study of ET in chiral linked systems reveals reasons for the various reactivities of chiral molecules, including the difference in therapeutic activity of drug enantiomers.

Keywords: chiral drugs, NSAID, linked systems, dyads, diastereomers, dimers, electron transfer, stereoselectivity, spin selectivity, CIDNP, fluorescence

1. Introduction: ET in the investigation of the binding of chiral drugs with biomolecules

Chiral systems are in the top of interest for a long time to this day. From the chemical point of view, the most interesting are the following issues: sources of the chiral biomolecules appearance in prebiological period, and physicochemical reasons of the difference in biological and medical activity of enantiomers. It is a matter of debate up to now [1]. On the both directions, significant progress has been made in the last decade of the twentieth century and the beginning of the twenty-first century. This review will focus on elementary ET process in chiral systems. These systems are donor-acceptor dyads with two chiral centers studied by spin chemistry and photochemistry methods. Similar dyads are frequently used to simulate the binding of chiral drugs with receptors or enzymes [2, 3]. They are diastereomers, where one partner is a drug enantiomer. Such systems attract attention since drug enantiomers demonstrate different, often just opposite, medical activity. It is a practical problem of pharmacology and medicine [1].

Despite this, numerous biochemical studies did not give a definite answer about the reasons for the difference in enantiomer medical activities.

Because enantiomers have identical physicochemical properties, there are no physical reasons of the difference in reactivity. But in active sites of enzymes and receptors, chiral enantiomers interact with chiral amino acid residues, and it lets us expect that drug-enzyme or drug-receptor complexes will be similar to diastereomers. If binding process includes stages with charge transfer, the ET in dyads would be a convenient model to simulate drug-receptor or drug-enzyme interaction. Suggested approach is based on two major assumptions. First, it is suggested that the reactivity of active intermediates would not depend on their generation pathway. Second, using photoirradiation instead of enzymatic one for the studied processes, activation is possible since an activation barrier is decreased as a result of increasing of drug's oxidation potential in its excited state [3].

ET in chiral systems is studied by the example of nonsteroidal anti-inflammatory drugs (NSAIDs), medicines that demonstrate remarkable difference in enantiomers medical activity [1, 4]. PET was studied by the UV irradiation of dyads including NSAIDs linked by bridges with various electron donors [5–10]. The exploration by using fluorescence and laser flash photolysis has shown that ET in dyads is stereoselective.

The application of photochemistry and CIDNP methods to study dyads with known representative NSAID naproxen (NPX) and donors N-methylpyrrolidine (Pyr) and tryptophan (Trp) has shown that, under the UV irradiation, partial and full charge transfer occur. Both processes demonstrate stereoselectivity [3, 11–14].

This difference in reactivity of (S)- and (R)-NPX isomers, which are part of diastereomers, is in qualitative agreement with some results of biochemical research [3]. So, (R)-isomer is more active in cytochrome P-450-induced metabolism that involves stage of ET. At that, indeed, the rate constant of the local excited state transition to a state with partial charge transfer systematically is greater for (R,S)-diastereomers. If we imagine that the process of partial charge transfer leading to exciplex formation can simulate the binding process, then large quantum yields of exciplex fluorescence for (S,S)-diastereomers compared with (R,S)- will mean the better binding of (S)-NPX with a donor.

The following peculiarity of ET process in chiral systems is spin selectivity [15]. Spin selectivity means the difference in CIDNP effects of dyad diastereomers, shown by the example of two dyads: NPX linked by a rigid bridge with the donor Pyr, and NPX-Trp dyad. Spin selectivity appearance lets us assume the difference in electron density distribution of (R,S)- and (S,S)-dyad diastereomers.

Thus, the above results have shown that full ET and partial charge transfer processes play a significant role in understanding of chiral systems reactivity.

Further, this chapter will be devoted to the description of two features of ET in chiral systems: stereo- and spin selectivity and the influence of environment on these peculiarities.

2. Stereoselectivity of PET in chiral dyad diastereomers

In this part, we will discuss the appearance of stereoselectivity of processes with PET in the linked systems with different NSAIDs.

2.1 Linked systems with flurbiprofen

Photoinduced interactions of (S)-/(R)-flurbiprofen (FBP) and thymidine (dThd) were studied in covalent-linked systems in work [5] (for structures,

see **Figure 1**). Under the illumination of (R)-FBP-dThd and (S)-FBP-dThd solutions in aerated acetonitrile, chromophore $^1\text{FBP}^*$ was excited and its fluorescence quantum yield (ϕ_f) and lifetime (τ_f) values were smaller than those of free FBP in solution. Authors suggested this dynamical quenching carries out through ET (where FBP is a donor) or exciplex formation. This theory is supported by Gibbs energies (ΔG) estimation in solutions of different polarity (acetonitrile and dioxane) by using classical Rehm-Weller-Zacharias criterion [16]. This criterion application has demonstrated that both partial and full charge transfer are possible in acetonitrile but exciplex formation is prevailing in dioxane. Fluorescence quantum yields and lifetimes have shown stereoselectivity of these processes—for (R)-isomer, ϕ_f and τ_f (0.015 and 0.27 ns) were smaller than for (S)- (0.018 and 0.31 ns).

For systems with amino acid Trp (structures in **Figure 2**), stereoselectivity of quenching process was also demonstrated. In this case, the excitation wavelength 266 nm was chosen where about 60% of light is absorbed by FBP and 40% by Trp, respectively. Significant fluorescence quenching was detected, and residual spectrum was referred to Trp chromophore. Also wide exciplex band was registered (380–500 nm), and its lifetimes for (R,S)- and (S,S)-isomers revealed the biggest stereoselectivity—5.1 and 7.6 ns (in N_2 bubbled acetonitrile solutions), respectively. As for fluorescence quantum yields and lifetimes of the main spectrum band attributed to the dyad excited state, the values were ϕ_f (R,S) = 0.02, ϕ_f (S,S) = 0.04; τ_f (R,S and S,S) = 0.9 ns. Possibility of electron transfer and exciplex formation was checked by ΔG values estimation (using Rehm-Weller-Zacharias equation [16]), in both cases processes turned out to be exergonic [6].

For systems with amino acid tyrosine, some stereoselectivity of photoinduced charge transfer was also found and, in this case, main attention was focused on the influence of spacer between partners [7]. One system FBP-Tyr had flurbiprofen and tyrosine connected directly, and another one had them separated by a cyclic spacer (see **Figure 3**).

As in previous flurbiprofen systems, these systems were studied by means of time-resolved fluorescence and flash-photolysis spectroscopy in acetonitrile solutions. Significant fluorescence quenching was found for both systems with short and cyclic bridge. It was attributed to electron transfer. Expectedly, this process was more efficient for the system with short bridge. Fluorescence quantum yields were 0.04 and 0.09 (for (R,S)- and (S,S)-FBP-Tyr, respectively), 0.15

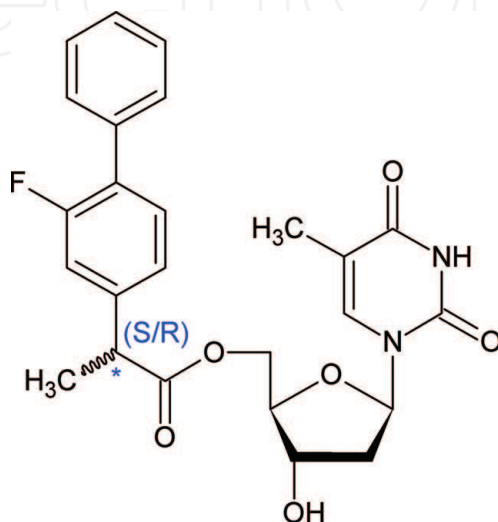
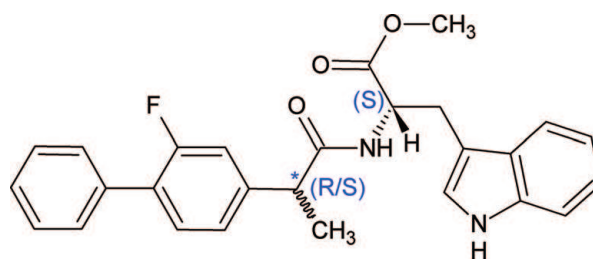
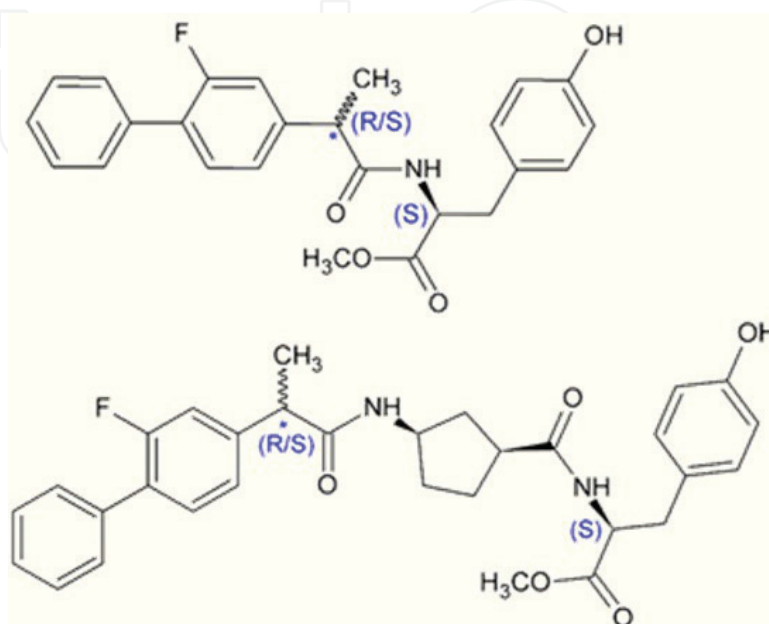


Figure 1.
Chemical structures of FBP-dThd dyads.

**Figure 2.**

Chemical structures of (R)-/(S)-FBP-Trp dyads.

and 0.11 (for (R,S)- and (S,S)-FBP-CyAA-Tyr). Average fluorescence lifetimes were 0.36 and 0.9 ns (for (R,S)- and (S,S)-FBP-Tyr, respectively), 1.2 and 0.93 ns (for (R,S)- and (S,S)-FBP-CyAA-Tyr). Interestingly, that for systems with a cyclic spacer exciplex formation was registered in fluorescence spectra and its lifetimes were 3.05 ± 0.01 and 3.27 ± 0.01 ns for (R,S)- and (S,S)-FBP-CyAA-Tyr, respectively. Possibility of electron transfer and exciplex formation was confirmed by authors with ΔG values estimation (by using Rehm-Weller-Zacharias equation [16]). Even more stereodifferentiation was observed for these systems triplet state: 0.14 and 0.27 (for (R,S) and (S,S)-FBP-Tyr), 0.39 and 0.22 (for (R,S) and (S,S)-FBP-CyAA-Tyr). No stereoselectivity was detected at early times, only after about 10 ps. The kinetics of (R,S)-FBP-Tyr was found to decay faster than its (S,S)-analogue after 10 ps; on the contrary, for the dyads with rigid bridge, the opposite behavior was observed [8]. These differences were analyzed in view of conformational peculiarities of studied systems. Computations have shown that geometrical arrangement of FBP and Tyr was favored for donor-acceptor interaction in (R,S) with short bridge due to its folded conformation, which was in agreement with fluorescence data. And geometry of this dyad (S,S)-configuration was more distorted, and fluorescence quenching was less efficient. Concerning dyads with rigid bridge, authors claimed more unfavorable geometry for interaction, especially for the (R,S)-diastereomer, where the two chromophores are practically in orthogonal arrangement. That is also in line with (R,S)- lower fluorescence quenching compared to (S,S)-FBP-CyAA-Tyr. Exciplex formation was not analyzed in these computations.

**Figure 3.**

Chemical structures of FBP-Tyr (top) and FBP-CyAA-Tyr (bottom).

2.2 Linked systems with carprofen

Chiral systems photoinduced interactions with amino acids were also studied in work [9]. In this case, an acceptor role is played by another NSAID—carprofen (CPF-Trp, see systems structure in **Figure 4**) and a donor amino acid was tryptophan (in dyad and in human serum albumin).

In the presence of albumin in the solution of CPF, similar transient absorption spectra were observed for both CPF stereoisomers. However, time-resolved measurements have shown significant difference—for each isomer, triplet state quenching profile had two components with different lifetimes. Authors corresponded these times to CPF complexation with two possible albumin bonding sites (site I and site II). This mapping was confirmed in experiments with another NSAID—ibuprofen as a substitute in site II. Therefore, shorter components, which had shown more significant stereodifferentiation ($\tau_R/\tau_S \sim 4$), were associated with CPF triplet state in site I; and lifetime shortening authors linked with excitation quenching by charge transfer from only one possible partner in protein—Trp amino acid residue. Laser flash photolysis study of model linked system—CPF-Trp dyad (**Figure 4**) confirmed this idea. Trp cation-radical was registered (with absorption maximum at ~ 580 nm); this is the evidence of electron transfer mechanism. And triplet lifetimes of model systems demonstrated stereodifferentiation— $\tau_{RS} = 2.4 \mu\text{s}$ and $\tau_{SS} = 3.0 \mu\text{s}$. Interestingly, that in this case, in opposite to all flurbiprofen-contained dyads, no reactivity was observed for singlet excited state—all fluorescence quantum yields and lifetimes were equal to carprofen itself $\phi_{fl} = 0.068$ and $\tau_{fl} = 1.55$ ns.

Another study involving drug in complex with α_1 -acid glycoprotein (BAAG) was performed by photophysical methods [10]. Laser flash photolysis in solutions of BAAG/(S)-CPFMe (methyl ester of carprofen) and BAAG/(R)-CPFMe in proportion 2:1 was performed and decay traces have shown stereodifferentiation. Thus, the triplet lifetime value for the (S)-enantiomer was much shorter ($13 \mu\text{s}$) than that of (R)-analogue ($18 \mu\text{s}$). Authors proposed that this could be related to the more efficient quenching of triplet excited state $^3\text{CPFMe}^*$ by electron transfer from Trp in the case of (S)-CPFMe, which is in agreement with a closer distance from (S)-CPFMe to a Trp residue than in case of (R)-CPFMe, within the binding site pocket [9].

2.3 Linked systems with naproxen

NSAID NPX as a part of linked systems with electron donors was studied in many works. Interestingly, system with NPX was dyad NPX-oxetane (OXT) (**Figure 5**) [17]. Illumination of systems in acetonitrile and chloroform solutions at NPX absorption wavelength (300 nm) led to ring opening.

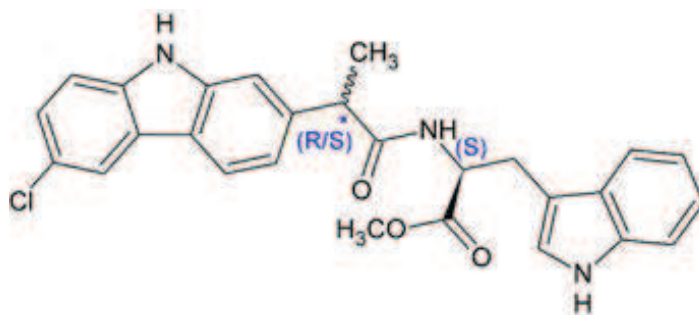


Figure 4.
Chemical structures of dyads (R)-/(S)-CPF-Trp.

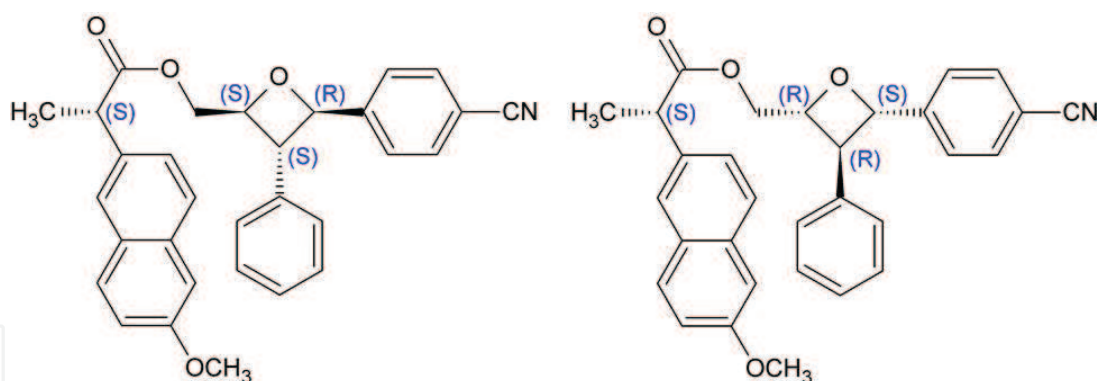


Figure 5.
Linked systems structure: left—(S)-NPX-(S,R,S)-OXT, right—(S)-NPX-(R,S,R)-OXT.

Authors explained this reaction mechanism also by involving photoinduced electron transfer (reaction scheme is presented in **Figure 6**).

Interestingly, that high reactivity was observed in acetonitrile but high stereoselectivity was in chloroform ($\tau_{S,R,S}/\tau_{R,S,R} \sim 1.5$). Allegedly, this is because of twisted conformations that prevail in dyad (S)-diastereomer. In this conformation, naphthalene fragment oriented to oxetane that favors intramolecular electron transfer [17].

More detailed investigation of processes with partial and full charge transfer in linked systems was performed by examples of several dyads from **Figure 7** [3, 11–14].

In this case, besides using time-resolved fluorescence measurement, CIDNP method has been applied to detect the state with full charge transfer between donor and acceptor—biradical-zwitterion (BZ) formed as a result of intramolecular ET.

CIDNP is phenomenon that manifested as unusual NMR signals, with the population of nuclear spins different from Boltzmann population. These signals are observed in the products of radical reaction, carried out directly in the probe of NMR spectrometer. There are singlets and multiplets with enhanced absorption or emission existing for a short time comparable with time of nuclear relaxation. These effects are the result of weak magnetic interactions in the radical pair (RP), which is a precursor of products. In essence, CIDNP, formed in high magnetic field of NMR spectrometer, reflects the difference in the recombination probability of RPs with α_N and β_N nuclear spin projections on the magnetic field direction. It depends on hyperfine coupling constants, the difference in g-factors of two radicals in RP, multiplicity of the RP precursors, the type of reaction, and some other parameters [18]. Today, CIDNP is the most direct method for detecting paramagnetic precursors of radical reaction products.

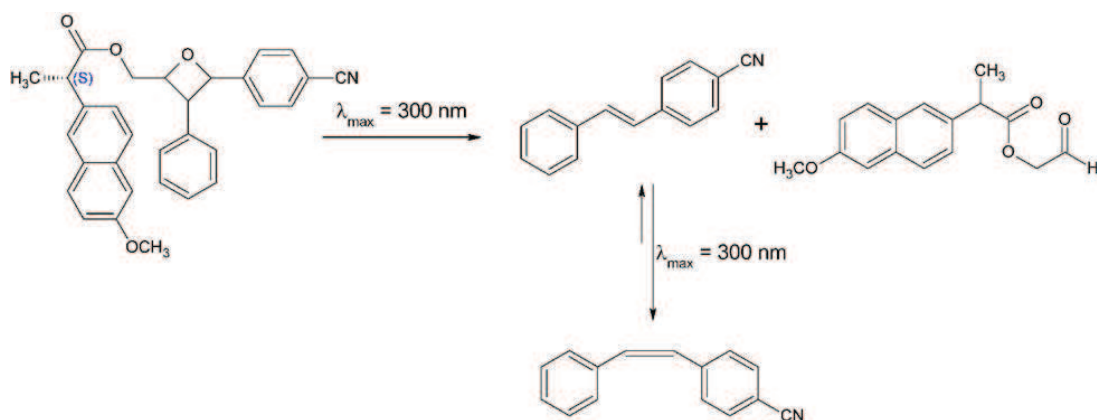


Figure 6.
Scheme of photoinduced ring opening in systems (S)-NPX-(S,R,S)-OXT and (S)-NPX-(R,S,R)-OXT.

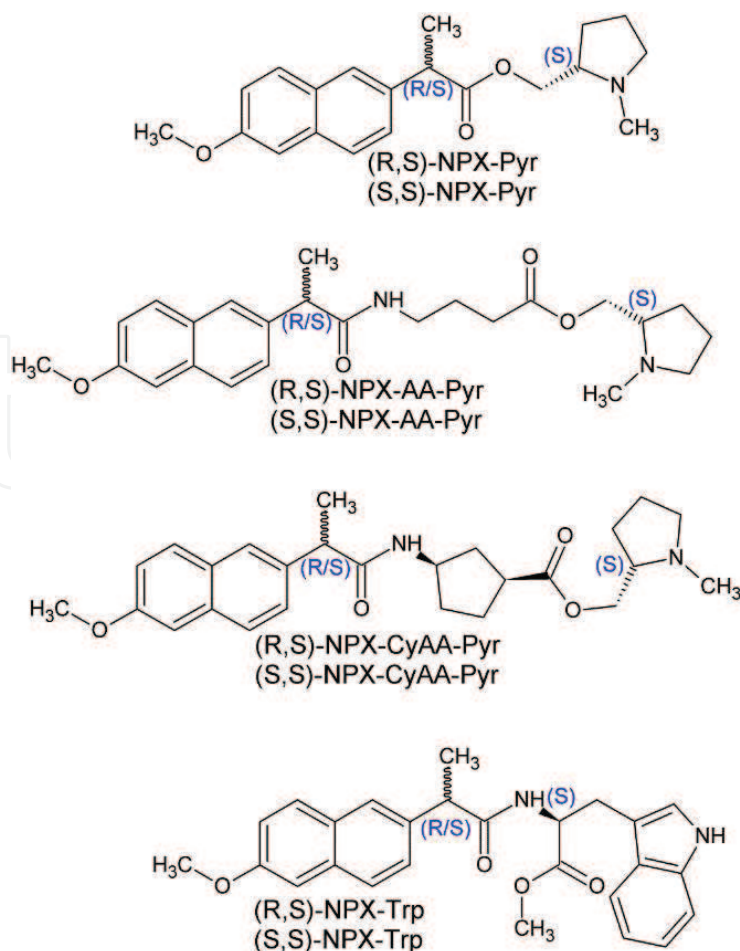


Figure 7.

Linked system structures: NPX-Pyr—“short,” NPX-AA-Pyr—“flexible,” NPX-CyAA-Pyr—“rigid,” and NPX-Trp—“tryptophan dyads.”.

The formation of BZ under the UV irradiation of dyads pictured in **Figure 7** was detected using CIDNP [3]. In accordance with spin density distribution in BZ, maximal CIDNP effect demonstrates methyl protons of N-methylpyrrolidine group (**Figure 8**).

The same CIDNP effects have demonstrated all other dyads with donor N-methylpyrrolidine. Unlike the mentioned dyads, diastereomers of dyad NPX-Trp have shown CIDNP of both aromatic and aliphatic protons (**Figure 9**).

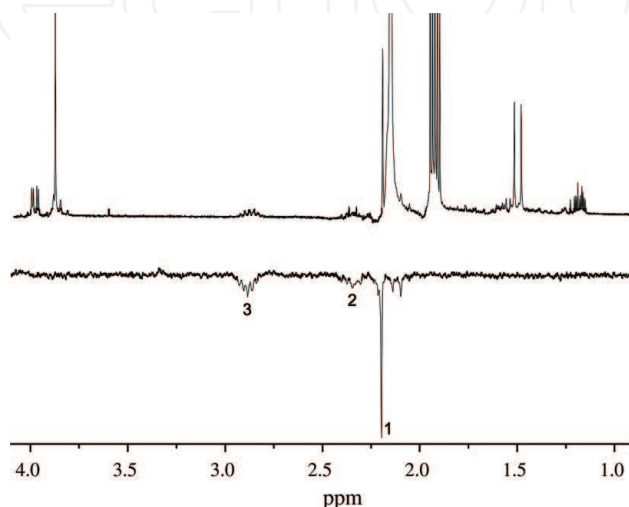


Figure 8.

NMR and CIDNP spectra detected after laser irradiation of (S,S)-NPX-Pyr “short” dyad in CD_3CN ; 1—N- CH_3 , 2—CH, 3— CH_2 signals of α protons in N-centered radical-cation of N-methylpyrrolidine fragment.

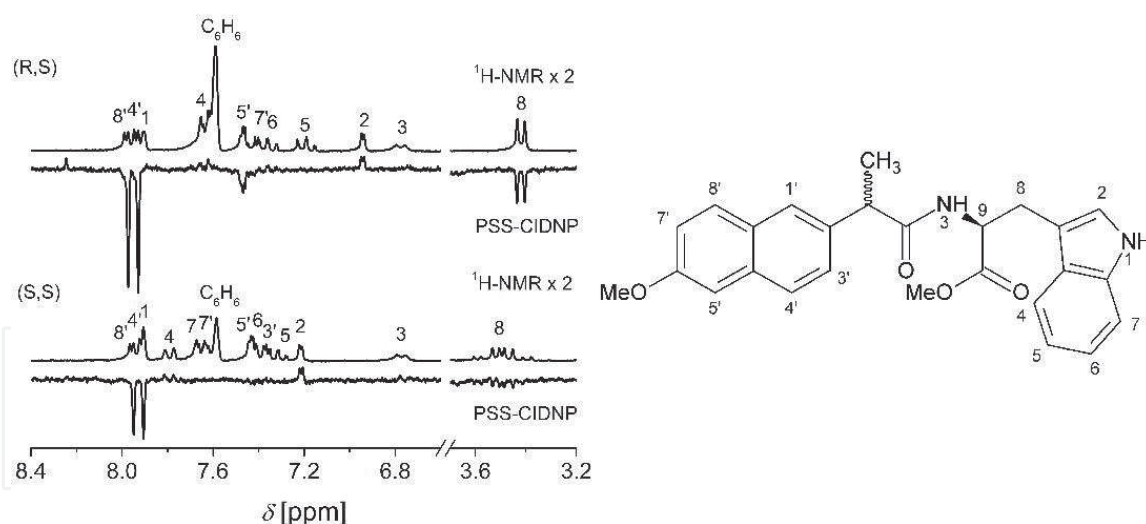


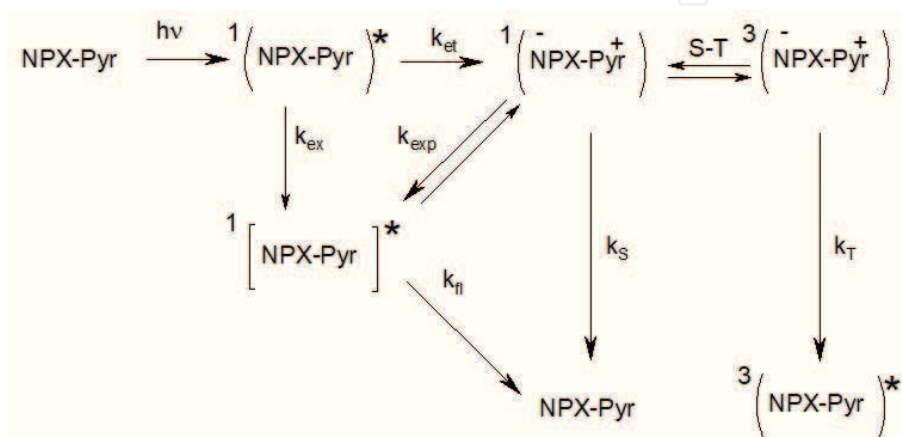
Figure 9.

NMR and pseudo steady state (PSS) CIDNP spectra of dyad's NPX-Trp solutions (5 mM in 40% C_6D_6 , 0.17% H_2O , the rest is CD_3CN): (R,S)-top, (S,S)-bottom. Reproduced with permission from Ref. [11] © John Wiley & Sons, Ltd., 2018.

The reason of the distinction of CIDNP pattern in dyads with N-methylpyrrolidine and Trp relates with the difference in the ratios of HFI constants in paramagnetic centers of donor and acceptor. In the case of NPX-Trp dyad, HFI constants of both fragments are the same order of magnitude, so CIDNP effects are appeared on all groups of protons. As it was mentioned above, in BZs of dyads with Pyr HFI constants of α protons in pyrrolidine fragment prevail; therefore, they determine the singlet-triplet evolution in RP.

Thus, CIDNP spectra in all studied dyads point at NPX excited state quenching via ET, followed by the formation of BZ (**Scheme 1**). CIDNP signs analysis carried out according to the known rules of R. Kaptein modified by G. Closs showed that the singlet excited state of dyads is quenched by an electron donor in intramolecular process [18]. An intramolecular ET is favored since a difference in order of magnitude between the rates of monomolecular and bimolecular quenching: $W_{intra} = 2-8 \times 10^8 \text{ s}^{-1}$ and $W_{inter} = 2 \times 10^9 \times 5 \times 10^{-3} = 10^7 \text{ M}^{-1} \text{ s}^{-1}$ [11, 12, 14].

Well-known criterion of Rehm-Weller-Zacharias points at the possibility of the back ET from both singlet and triplet spin states of the BZ [12, 16]. According to this criterion, ET for studied systems is possible if the value of free energy (ΔG) is negative $\Delta G = [E_{ox}(D/D^+) - E_{red}(A^-/A)]\epsilon_0 - e/\epsilon a + \Delta G_{solv} - E(^{1,3}D^*)$. Here $\Delta G_{solv} = e^2/2(1/R^{D^+} + 1/R^{A^-}) \times (1/\epsilon - 1/\epsilon_0)$, $E_{ox}(\text{Pyr}) = 1.0 \text{ eV}$, $E_{red}(\text{2-methoxynaphthalene}) = -2.6 \text{ eV}$, and $E_{0-0}(\text{NPX}) = 3.69 \text{ eV}$.



Scheme 1.

Mechanism of NPX-Pyr singlet excited state quenching.

Since for NPX $E_T = 3.25$ eV and ΔH in BZ is equal to $E_{ox}(D/D^+) - E_{red}(A-/A)$ $\epsilon_0 = 3.6$ eV, then NPX in excited triplet state can be formed via the back ET in BZ of triplet collective spin state.

Thus, analysis of the CIDNP, detected upon the UV irradiation of studied dyads, allows one to confirm ET between (S)- and (R)-NPX and donors. Note, in the case of dyads with Pyr, CIDNP analysis using Kaptein rule [18] has shown that back ET occurs predominantly from the singlet collective spin state of BZ, whereas for the NPX-Trp dyad, it occurs mainly from the triplet spin state of the BZ [14].

According to the calculated curves in **Figure 10**, the experimental CIDNP dependences on dielectric constant in both cases of partial and full charge transfer should be smooth curves without extremes.

However, the experimental dependences of CIDNP for dyads with N-methylpyrrolidine on the dielectric constant are curves with maxima position, depending on the bridge length. Such shapes mean that the CIDNP effects are formed in at least two processes, and their contributions depend on the permittivity and dyad structures. Therefore, the resulting polarization has to be formed from the back ET in both singlet and triplet collective spin states of the BZ. According to CIDNP signs analysis, the rate constant of back ET in BZ singlet spin state (k_S) has to be higher than that for triplet state (k_T). Meanwhile, there are reference data informing that in the pair of amine radical-cation and naphthalene radical-anion, k_T value is higher than k_S [11, 12]. It is reasonable to assume that the predominance of k_S is related to the formation of a singlet exciplex, being in equilibrium with the BZ. The detailed mechanism of NPX singlet excited state quenching by the N-methylpyrrolidine, provided on the basis of CIDNP analysis, is shown in **Scheme 1**.

So, CIDNP analysis points that NPX excited state quenching in above dyads goes through stages of full and partial charge transfer. Details of the processes of partial charge transfer: rate constants of local excited state (LES) and exciplex accumulation and decay and exciplex fluorescence quantum yields were obtained from fluorescence measurements, including time-resolved experiments.

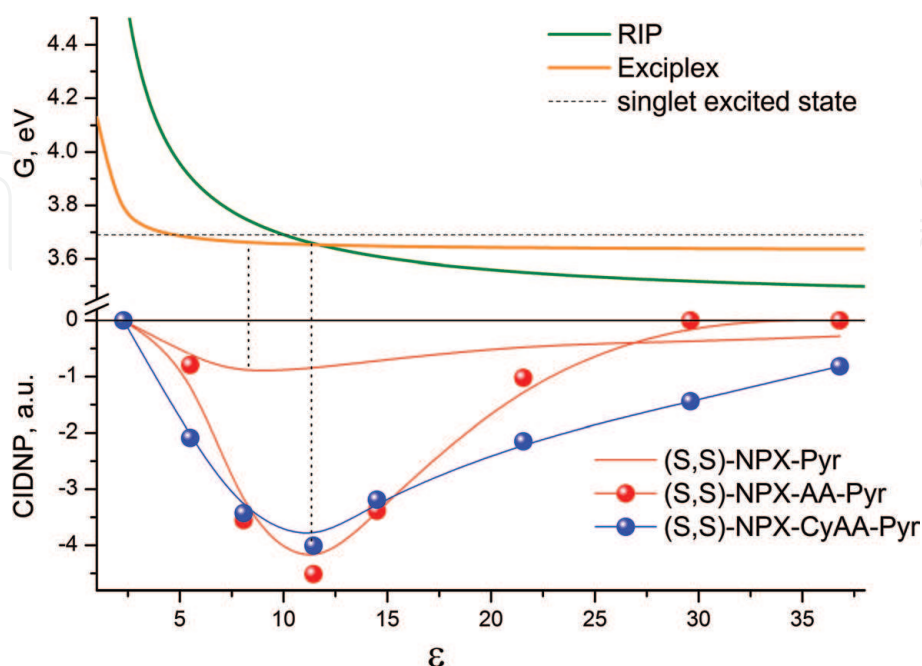


Figure 10. Dependence of free energies of the radical-ion pair of N-methylpyrrolidine radical-cation and methoxynaphthalene radical-anion on solvent permittivity, calculated using Rehm-Weller-Zacharias equation and dependences of CIDNP on solvent permittivity for short, flexible, and rigid dyads (bottom). Reproduced from Ref. [3] with permission from the PCCP Owner Societies.

The fluorescence spectra of dyad diastereomers with short, flexible, and rigid bridges compared with NPX methyl ether in acetonitrile are presented in **Figure 11**.

There are two emission bands; they refer to local excited state of NPX moiety (350 nm) and exciplex (520 nm). The decreasing of dyad fluorescence intensity was accounted for new quenching channel—transition from LES to exciplex [13]. Note that LES fluorescence quantum yield is higher for dyad with flexible bridge, whereas exciplex fluorescence quantum yield is higher for dyad with rigid bridge. At that, fluorescence decay traces of both LES and exciplex were approximated by two exponential models with short and long lifetimes for LES and rise and decay times for exciplex. Fluorescence spectra and kinetics of its quenching were investigated in solvents with different dielectric constants (**Figure 12**).

Careful analysis of fluorescence data allows authors [3] to suggest the existence of two fast equilibria: “exciplex—LES” and “exciplex—BZ”. In this work, the summary scheme of NPX chromophore quenching by electron donor was proposed (**Scheme 2**).

In this figure, two different dyad conformations in ground state, namely, expanded and folded, transfer to LES and exciplex through pathways W_1 and W_2 , respectively. The development of this mechanism is based on the kinetic curves fitting, considering that LES and the exciplex are formed simultaneously. According to Scheme 2, the exciplex exists in dynamic equilibrium with LES (k_4 , k_5) and BZ (k_7 , k_8). BZ, in turn, can be in singlet or triplet spin states that have equal energy. Spin conversion (k_{S-T}) occurs under the magnetic interactions in BZ. Back ET from both BZ spin states leads to the formation of parent dyad in singlet ground state and in triplet excited state (with corresponding rate constants k_S and k_T). Emission of LES and exciplex is determined by k_3 and k_6 rate constants. Exciplex also undergoes internal conversion with rate constant $k_{isc(exc)}$.

The kinetics of LES and exciplex fluorescence were calculated by solution of differential equation system using Runge-Kutta method [3], to obtain rate constants of separate stages. Thus, the values of quenching rate constants (k_3 – k_7) were obtained in [3]. It is remarkable that there is a difference between the values of diastereomers rate constants, in particular k_4 , k_7 , related with charge transfer processes (see **Figure 13**).

The greatest difference between the values of diastereomers k_7 (exciplex transformation into BZ) is observed only in polar media. At that, the constant k_4 (transition from LES to exciplex) is higher for (R,S)-diastereomers of all three dyads.

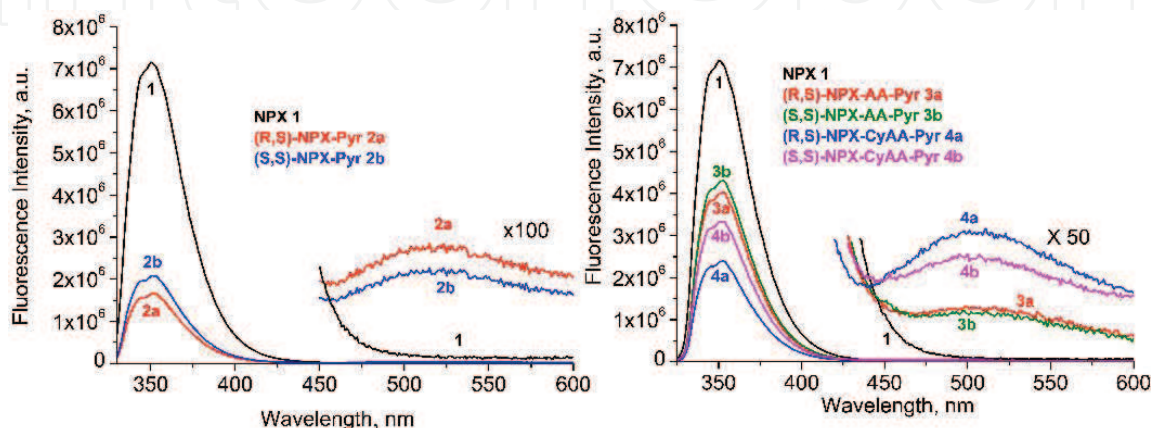


Figure 11.

Fluorescence spectra of (S)-NPX-OMe (1), (R,S)-NPX-Pyr (2a), and (S,S)-NPX-Pyr (2b), (R,S)-NPX-AA-Pyr (3a), (S,S)-NPX-AA-Pyr (3b), (R,S)-NPX-CyAA-Pyr (4a), and (S,S)-NPX-AA-Pyr (4b) in acetonitrile, excitation wavelength 320 nm. Magnified long-wavelength bands of exciplex are shown in insert.

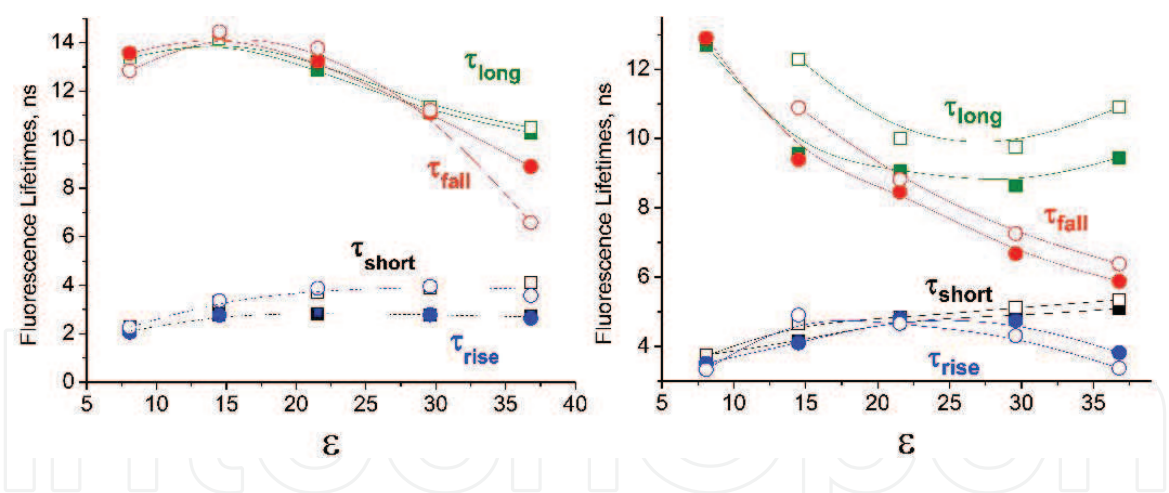
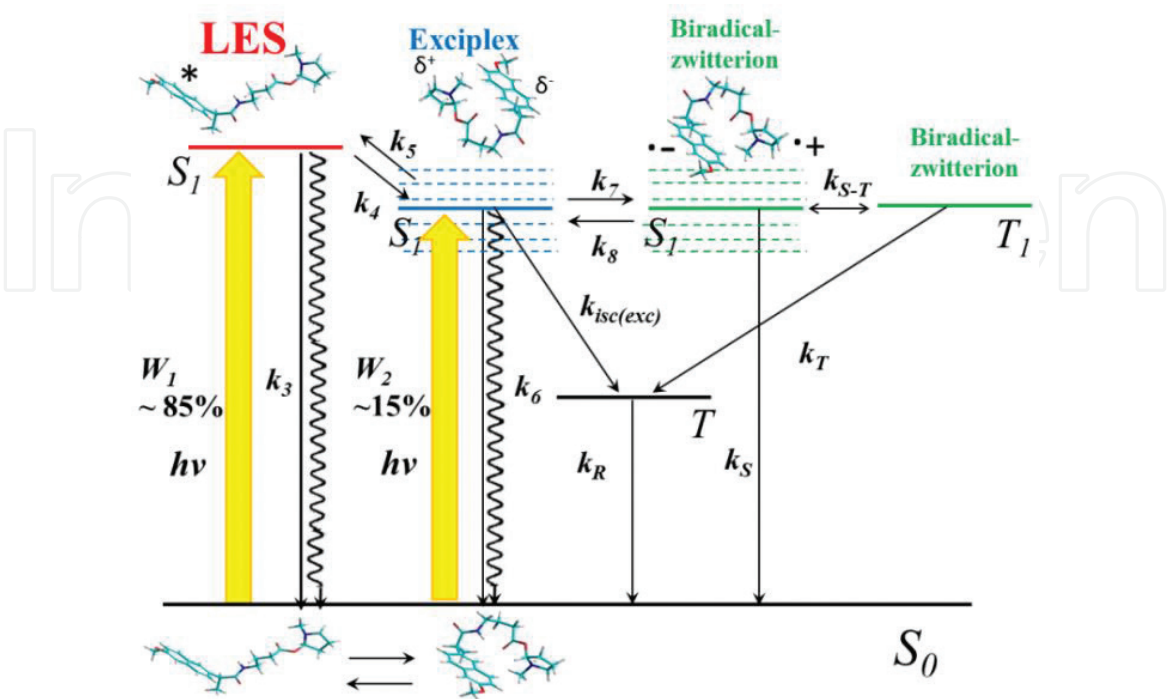


Figure 12. Dependences of fluorescence lifetimes for NPX-AA-Pyr dyad (left) and NPX-CyAA-Pyr (right). LES—squares (τ_{short} , τ_{long}), exciplex—circles (τ_{rise} , τ_{fall}), solid—(R,S)-diastereomers, open—(S,S)-diastereomers. Reproduced from Ref. [3] with permission from the PCCP Owner Societies.

Note that NPX-Pyr diastereomers were previously investigated by using fluorescence technique in work [19], where stereoselectivity was also revealed (τ_{fl} (RS) = 2.35 ns, τ_{fl} (SS) = 3.02 ns, rate constants of ET $k_{\text{RS}} = 2.8 \times 10^8 \text{ s}^{-1}$, and $k_{\text{SS}} = 1.8 \times 10^8 \text{ s}^{-1}$).

Thus, the appearance of stereoselectivity in ET was shown for a number of dyads. In particular, the stereoselectivity of the rate constants of separate stages of NPX excited state quenching was demonstrated by the example of dyads with donor N-methylpyrrolidine. The biggest difference is shown by rate constants of LES transfer to exciplex for (R,S)- and (S,S)-diastereomers of dyads with short bridge. The similar results were obtained for exciplex fluorescence quantum yields measured in solvents with different dielectric constants. So, the stereoselectivity in the systems under study significantly depends on the distance between the chiral centers and the structure of the bridge.



Scheme 2. Mechanism of NPX chromophore quenching in dyads with flexible and rigid bridges. Dashed lines denote the dependence of LES and exciplex energy levels on solvent polarity. Reproduced from Ref. [3] with permission from the PCCP Owner Societies.

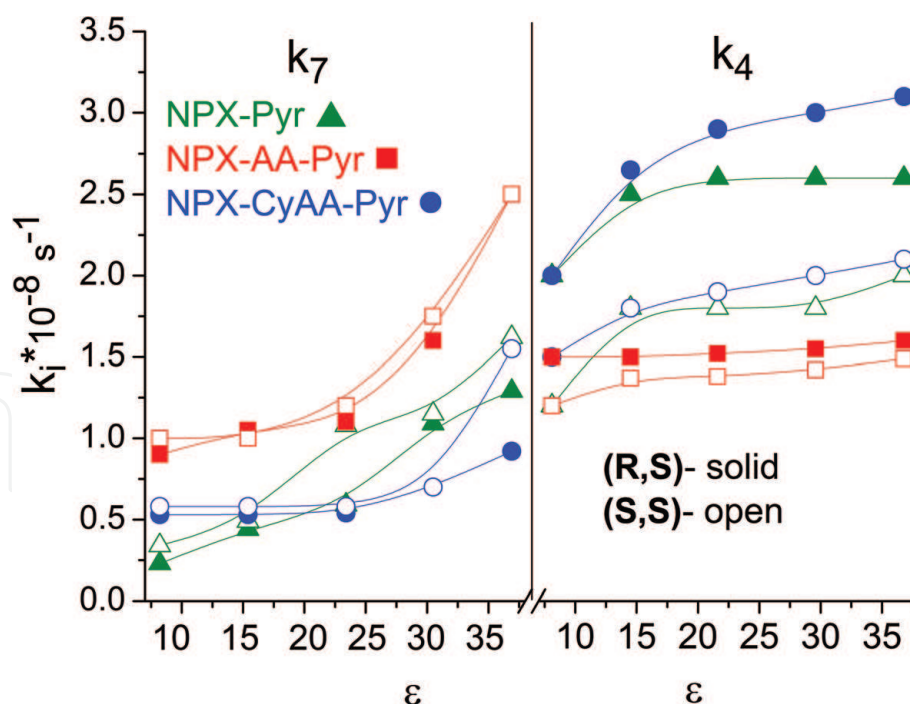


Figure 13.

Dependences of k_4 , k_7 rate constants on solvent polarity for three dyads linked with N-methylpyrrolidine. Reproduced from Ref. [3] with permission from the PCCP Owner Societies.

3. Spin selectivity: experiments and calculations

The following peculiarity of ET in chiral systems is spin selectivity. Spin selectivity implies the difference between CIDNP effects of dyad diastereomers, shown by the example of two NPX-based dyads: linked by rigid bridge with donor N-methylpyrrolidine, and linked with amino acid Trp (**Figure 7**).

This part of the chapter focuses on the application of CIDNP to study the difference of spin density distribution in diastereomeric BZs of abovementioned two dyads. For this purpose, in works [14, 15], the CIDNP effects in diastereomers of these dyads were compared.

Figure 14 represents the difference in the intensity of polarized signals of N-methyl protons in diastereomers of NPX-Pyr dyad.

Diastereomers of NPX-Trp dyad have demonstrated even greater distinction in CIDNP effects (see **Figure 8**, Section 2.3).

To study in detail the nature of differences in the CIDNP effects formed in BZs of these dyads, in work [15], so-called CIDNP enhancement coefficients per one paramagnetic particle were used.

For determination of the CIDNP enhancement coefficients per one paramagnetic particle, ratios of the intensities of polarized and equilibrium signals in the NMR spectra were divided by BZ concentrations, estimated from fluorescence data [3]. It should be noted that the extinction coefficients for two diastereomers are the same. Further, we will operate only with the ratio of enhancement coefficients determined as follows:

$$K = \frac{I_{pol}^{RS} \times I_{eq}^{SS} \times [BZ]_{SS}}{I_{eq}^{RS} \times I_{pol}^{SS} \times [BZ]_{RS}} \quad (1)$$

in which I_{pol} is the intensity of the polarized signals of the NPX-Trp aromatic protons at the 8'-position or the N-methyl protons of NPX-CyAA-Pyr (see **Figure 14**), I_{eq} is the equilibrium signal intensity of the same protons, detected before photoirradiation.

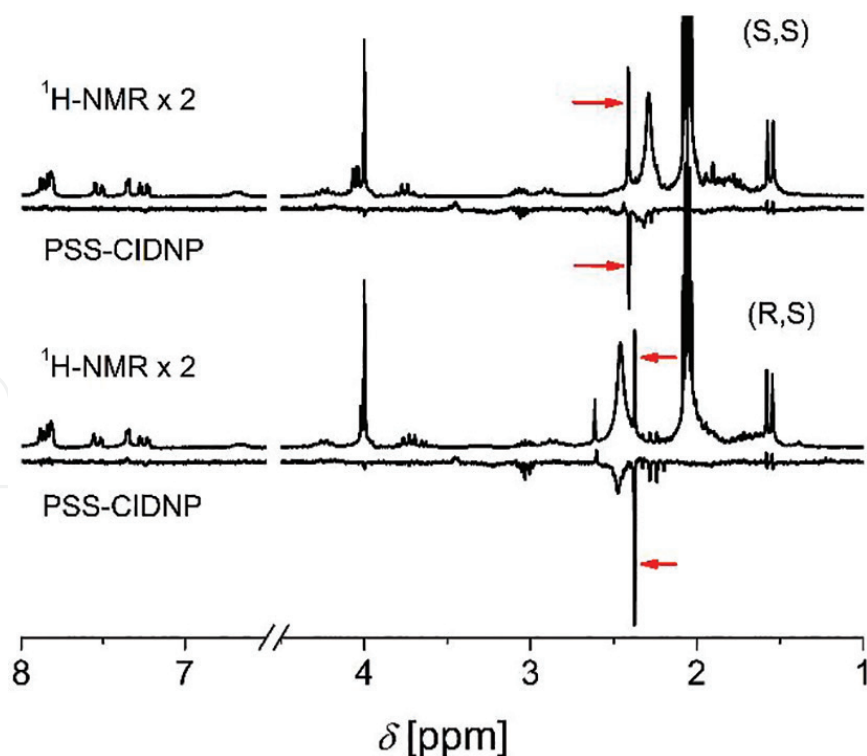


Figure 14. NMR and pseudo-steady-state (PSS) CIDNP spectra of NPX-CyAA-Pyr dyad diastereomers (5 mM) solution in CD_3CN (H_2O 0.05%): (S,S)—top, (R,S)—bottom. Negative polarized line situated at 2.3 ppm (red arrows) refers to N-methyl protons of dyad diastereomers. Reproduced with permission from Ref. [15] © John Wiley & Sons, Ltd., 2018.

As can be seen from figures, the CIDNP enhancement coefficients are appreciably higher for the (R,S)-diastereomers and the maximum ratio of enhancement coefficients, K , varies from 2.1 to 2.3 for both dyads. Since this is a polarization per one paramagnetic particle, the difference in the coefficients is certain to be the result of the distinctions in the magnetoresonance parameters of the (R,S)- and (S,S)-BZs. CIDNP effects for the diastereomers of NPX-CyAA-Pyr dyad were compared in acetonitrile, because in this case the contribution from exciplex to CIDNP effects is negligible and K values would be mainly determined by the magnetoresonance parameters of BZ (see **Scheme 1**). Further, to understand the origin of the differences in CIDNP enhancement coefficients in dyad diastereomers, these coefficients were calculated by varying the magnetoresonance parameters and lifetimes of BZ for NPX-CyAA-Pyr diastereomers. The calculation was carried out in the frame of radical pair theory by using two-position model and Green function method [15, 18]. According to this model, two states of the system are available. One is the state of a direct contact; the radicals are located in the reaction zone with characteristic time τ_r . The other is the state where the radicals are out of the reaction zone. The overall system lifetime is τ_c . Time that the system spends in the reaction zone (τ_r) is much less than the total lifetime of the system (τ_c). Calculations of CIDNP dependence on the HFI constant under various values of Δg and characteristic times (τ_c) were carried out. Next, authors tried to trace what variations of the abovementioned parameters could give the required adjustment—a twofold change in the CIDNP effects of diastereomers. The dependence of CIDNP on the hyperfine coupling constant is known to be bell-shaped for long-lived radical ion pairs [18]. The location of the dependence extremum is defined by the ratio of Δg and the hyperfine interaction constant. In the studied systems, we used the following BZ magnetoresonance parameters: $\tau_c = 10$ ns, whereas the experimental values are 7 and 9 ns for (R,S)- and (S,S)-diastereomers of NPX-CyAA-Pyr dyad, $\tau_r = 1$ ns, and $\Delta g = 10^{-3}$ [3, 20]. The latter is also the experimental value. From a comparison of

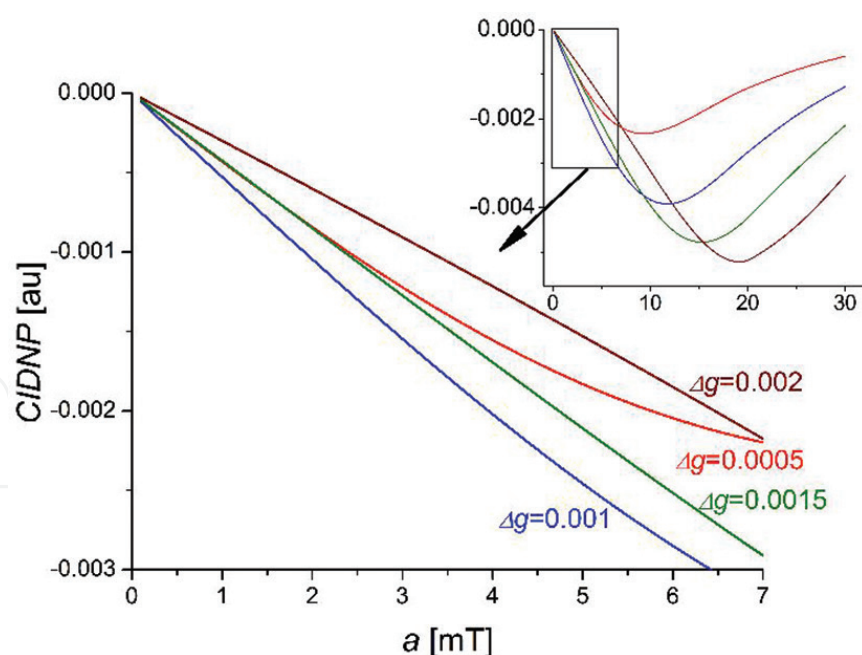


Figure 15.

Starting points and full curves (in insert) of the CIDNP intensity dependences on HFI constant values under $B = 4.7$ T, $\tau_r = 1$ ns, $\Delta g = 0.001$ and various τ_c . Reproduced with permission from Ref. [15] © John Wiley & Sons, Ltd., 2018.

the listed parameters, and by taking into account the bell-shaped CIDNP dependence, one can draw the following conclusion: because $2\Delta g H_0$ values are larger than hyperfine coupling constant values, greater polarization will correspond to a larger HFI constant. However, quantitative calculation can be carried out only for NPX-CyAA-Pyr dyad. In this case, the HFI constants of the N-methyl protons predominate in BZ, and therefore, one nuclear approximation can be applied for the calculations.

If we set the lifetime of $\tau_c = 10$ ns, which is close to the experimental values of 7 and 9 ns accordingly, $\tau_r = 1$ ns, and experimental value $\Delta g = 10^{-3}$, then it allows one to describe the difference observed in the values of CIDNP enhancement coefficients of NPX-Trp diastereomers. In this case, the values of hyperfine interaction constants for the (S,S)- and (R,S)-diastereomers differ by a factor of 2 (**Figure 15**). The same result will be achieved by proportional varying of Δg values. The changes required in the values of Δg factors are unlikely to be accepted as plausible. In addition to the variation of HFI constants and Δg factors, it is worthwhile to consider the influence of changes in characteristic lifetimes of the studied system. However, the experimental data points at much less than the required difference in BZ lifetimes.

Therefore, it seems reasonable to associate changes in the CIDNP enhancement coefficients of NPX-CyAA-Pyr diastereomers with the variation in HFI constants. Moreover, this conclusion is in accordance with the reference data [21–23]. EPR investigations of chiral stable radicals and biradicals revealed changes in the HFI constants of 1.5 and 2.

4. Spin selectivity and chiral catalysis

Another peculiarity of CIDNP in chiral systems is the dependence of enhancement coefficient ratios for (R,S)- and (S,S)-configurations on the ratios of diastereomer concentrations [15]. It was detected upon UV irradiation of diastereomers mixture of NPX-CyAA-Pyr dyad (**Figure 16**).

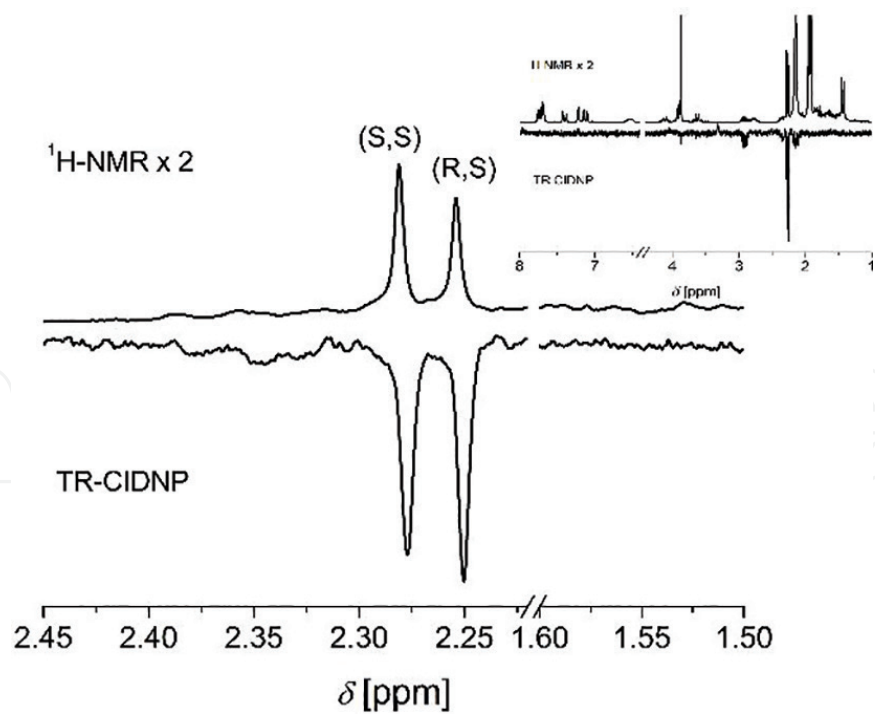


Figure 16. NMR and time-resolved (TR) CIDNP spectra of N-methyl protons area (full are presented in insert) detected in the mixture of NPX-CyAA-Pyr dyad diastereomers in acetonitrile (the ratio of (R,S)-/(S,S)- = 0.8). Reproduced with permission from Ref. [15] © John Wiley & Sons, Ltd., 2018.

The *K* values obtained for different ratios of diastereomers concentrations are presented in **Table 1**. The noticeable changes in the coefficient ratios, *K*, are visible. These changes in the *K* values obtained for different ratios of diastereomers concentrations point to the contribution of some intermolecular processes to CIDNP formation. The reference data on the tendency of substituted naphthalenes, including naproxen, to association [24–26] forces authors to suggest that the abovementioned intermolecular process might be the association of dyad diastereomers in solution—most likely, dimer formation. Since the studied dyads contain “naproxen” part and “tails”—the donor groups and bridges, including amide fragment -C(O)NH-, they can form associates due to the hydrogen bonds between amide groups of two molecules, specifically H-bond between amide group of one molecule and carbonyl or carboxyl oxygen of another one (**Figure 17**). XRD analysis in the solid state of NPX-Trp dyad diastereomers confirmed such H-bond formation [15].

Ratio of (R,S)/(S,S) concentrations	<i>K</i>
0.4	1.70 ± 0.09
0.7	1.80 ± 0.09
0.8	1.80 ± 0.09
1.0	1.9 ± 0.1
1.3	2.0 ± 0.1
1.8	2.3 ± 0.1
2.1	2.3 ± 0.1
2.3	2.3 ± 0.1

Reproduced with permission from Ref. [15] © John Wiley & Sons, Ltd., 2018.

Table 1. *K* values of NPX-CyAA-Pyr dyad diastereomers (column 2) determined for the different ratios of diastereomer concentrations (column 1)

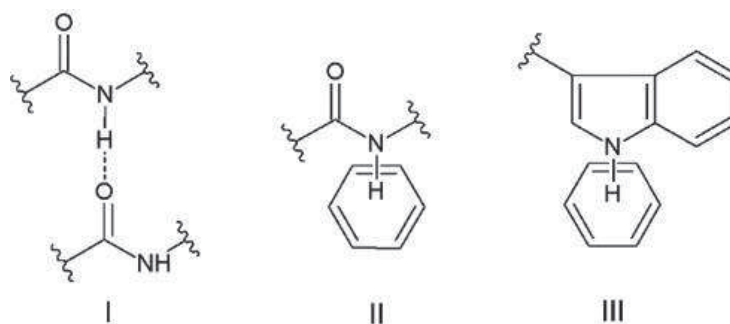


Figure 17. Self-associated (I) and collision complexes (II and III) of dyads with aromatic solvents. Reproduced with permission from Ref. [15] © John Wiley & Sons, Ltd., 2018.

As for the manifestation of the dyads association in solutions, dependences of both chemical shifts and the lines widths of diastereomers on the solvent composition, demonstrated in work [15], also indicate at the possibility of association. According to the reference data, it might be not only dimers (I), but the collision complexes of amide group and indole ring with aromatic solvents (II,III) (**Figure 17**).

Besides, the line widths of amide groups NH protons for both dyads showed the selective broadening (**Figure 18**).

These broadenings, along with chemical shifts solvent dependence, were referred to the slow exchange between monomers and dimers of dyads (**Scheme 3**, the first equilibrium) and to the solvation of dyads via H-bond formation (**Scheme 3**, the second equilibrium) [15].

On the other side, the fraction of the dyad associates and weak collisional complexes in acetonitrile and benzene mixture may vary depending on the ratios of components in the mixture. Then, we can assume that processes in solution would be different for (R,S)- and (S,S)-optical configurations of the dyads and might result in the *K* value variation in different solvents, accordingly.

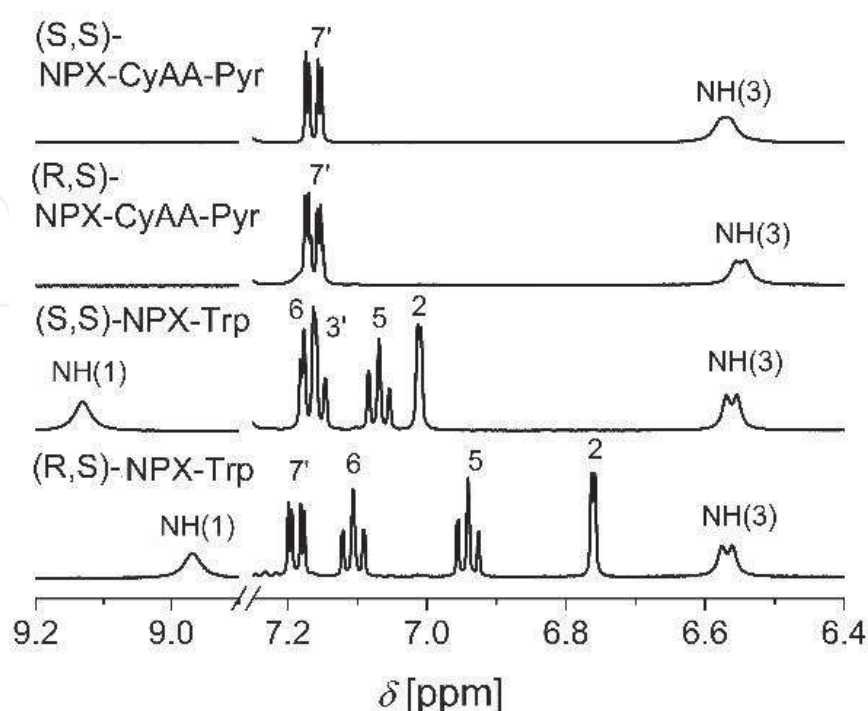
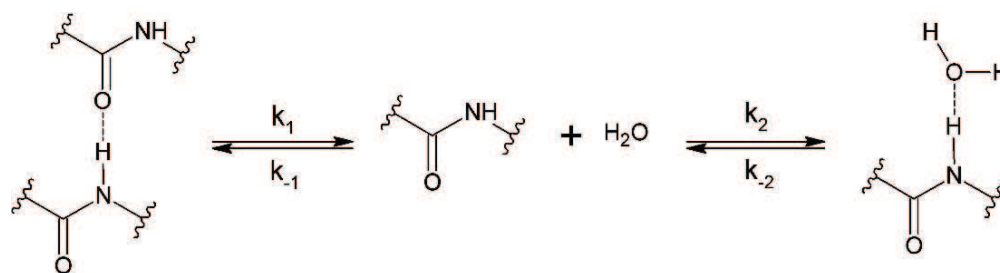


Figure 18. NMR spectra (the region of aromatic protons) of (R,S)-/(S,S)-NPX-Trp and (R,S)-/(S,S)-NPX-CyAA-Pyr dyads in the solvent mixture: $\text{CD}_3\text{CN} + 0.17\% \text{H}_2\text{O}$. Reproduced with permission from Ref. [15] © John Wiley & Sons, Ltd., 2018.



Scheme 3.

Possible ways of the participation of amide fragment of studied dyads in H-bond formation.

The impact of solvent on CIDNP coefficients of diastereomers was studied in work [15] on the example of NPX-Trp dyad, known not to form exciplex upon the UV irradiation. For this dyad, the minimal ratio of CIDNP enhancement coefficients of diastereomers is observed in acetonitrile 1.4 ± 0.1 . The presence of benzene in the mixture provides a large difference between the CIDNP of diastereomers, and this difference grows with the increasing of water concentration in solvent mixture (volume fraction % $\text{CD}_3\text{CN}/\% \text{C}_6\text{D}_6/\% \text{H}_2\text{O}$): 1.5 ± 0.1 (19.9/80/0.1) $< 1.7 \pm 0.1$ (59.8/40/0.2) $< 2.0 \pm 0.1$ (79.7/20/0.3). To explain the distinctions in K values in the different solvents mixtures, in work [11], several circumstances were taken into account: first, the capacity of the amide fragments for self-associating in polar solvents (**Figure 17, I**), such as acetonitrile, and second, the formation of collision complexes with aromatic compounds (**Figure 17, II and III**), including benzene [27].

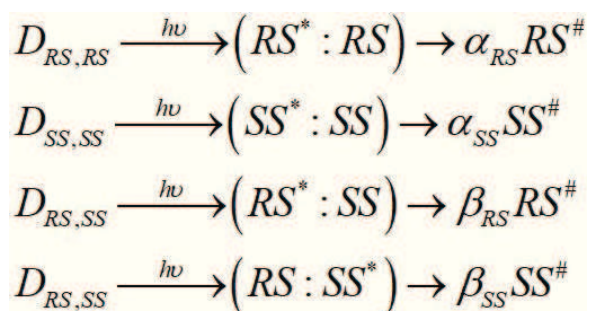
So, the difference in the solvent effects, that is, the association of optical isomers or formation of collisional complexes, can lead to distinctions in the BZ conformations. The latter also assumes the difference in the efficiency of singlet-triplet conversion that is responsible for CIDNP formation and magnitudes of diastereomers enhancement coefficients.

Further study of the effect of association on charge transfer processes in chiral dyads was undertaken in work [15]. Authors, in order to confirm the relation of K values dependence on (R,S)- and (S,S)-concentration ratios with dimers formation, calculated the dependence of K values on diastereomer concentration ratios in the frame of Frank theory of chiral catalysis [28].

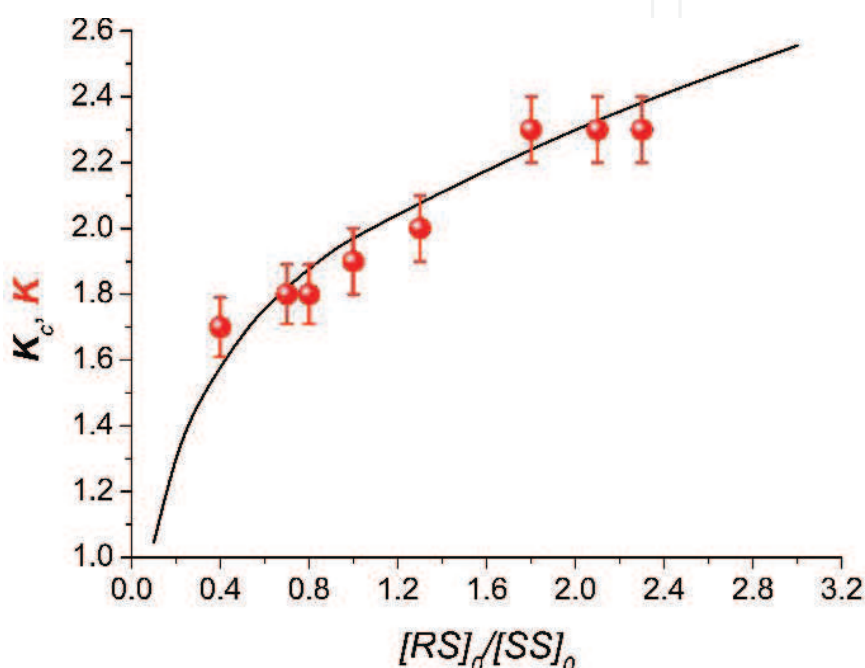
Frank theory is one of the most accepted theories among chemists, in which it was mathematically shown that a small amount of one chiral compound could increase its own reproduction and suppress the formation of another optical isomer [28]. The main requirement of Frank conception is the following: to obtain one isomer's prevalence, the presence of a chiral associate, for example, (S,S), (R,R), and (R,S) dimers, in the reaction mixture, is needed. In this case, the driving force of chiral enrichment is the competition between the catalyzing action of one enantiomer on the formation of the same isomer, and the inhibition of the formation of another optical isomer. So, the formation of homodimers (S,S), (R,R) will lead to chiral enrichment with one isomer and heterodimer (R,S) does not.

So, in work [15], to prove that polarized dyad diastereomers are products of back ET in homo- and heterodimers (R,S)-(R,S), (S,S)-(S,S), and (R,S)-(S,S), it was shown how a different ratio of diastereomers changes the value of K . Below is the scheme, where CIDNP values, α and β , are proportional to back ET efficiency (**Scheme 4**).

By Frank concept, α_{RS} and α_{SS} are appreciably higher than β , and, according to the experimental data, α_{RS} is twice as high as α_{SS} . Concentration of dimers was believed to be considerably higher than concentration of monomers. The calculation of K values was carried out by using a quasi-steady-state approximation. On

**Scheme 4.**

Photoinduced processes, occurring in homo- ($D_{RS,RS}$, $D_{SS,SS}$) and hetero- $D_{RS,SS}$ chiral dyad dimers. Reproduced with permission from Ref. [15] © John Wiley & Sons, Ltd., 2018.

**Figure 19.**

Experimental dependence of CIDNP enhancement coefficients K (data from Table 1, red balls) and calculated K_c (black line) dependence on (R,S)-diastereomer concentration. $[SS]_0 = 10^{-3}$ M, $\alpha_{SS} = 10$, $\alpha_{RS} = 20$, $\beta_{RS} = 1$, $\beta_{SS} = 1$; $K_{RS} = 2 \times 10^5$ M $^{-1}$, $K_{SS} = 2 \times 10^5$ M $^{-1}$, $K_{RS,SS} = 1 \times 10^5$ M $^{-1}$. Reproduced with permission from Ref. [15] © John Wiley & Sons, Ltd., 2018.

account of the above assumption, the dimer's stability constants have to be about 10^5 M $^{-1}$ at the initial monomers concentration 10^{-3} M. For detailed description of calculations, readers are referred to work [15].

Figure 19 displays the calculated (curve) and experimental (red circles) dependences of CIDNP coefficient ratios on diastereomer concentration ratios.

The agreement of experimental and calculated K values confirms the impact of association on ET process in dyad's diastereomers. So, back ET occurs in BZs, being part of dimers. It might be the additional reason of HFI constants variation in BZ of (R,S)- and (S,S)-configurations, resulting from different conformations of BZs. Since the dimerization also changes ET efficiency, the impact of dyad's dimerization on back ET efficiency might be considered as an example of ET chiral catalysis.

5. Conclusion

So, this chapter shows that the set of dyads, including (R)/(S)-NPX and chiral partner, have demonstrated stereoselectivity—difference in ET rates

of diastereomers. The joint studies by spin chemistry and photochemistry techniques, including the time-resolved measurements of dyads with donor N-methylpyrrolidine, have shown the stereoselectivity of separate stages of NPX excited state quenching, LES, and exciplex quantum yields.

The scale of these differences was found to be influenced by the donor-acceptor properties of the partners and the length and structure of the bridge. Another peculiarity of ET—spin selectivity was observed on the example of two NPX-based dyads. It is the different CIDNP effects formed via back ET in BZ of diastereomers. Spin selectivity is explained by the difference between HFI constants, which, in turn, determine back ET in BZs of (R,S)- and (S,S)-configuration. The impact of dyad's dimerization on ET efficiency might be considered as the first example of chiral catalysis in elementary process—ET.

Acknowledgements

This work was supported by the Russian Science Foundation (grant no. 18-13-00047). The authors are truly grateful to Prof. Plyusnin who contributed a lot to the work of Russian scientists.

Author details


Aleksandra Ageeva¹, Ekaterina Khramtsova^{1*}, Ilya Magin¹, Nikolay Polyakov¹, Miguel Miranda² and Tatyana Leshina¹

¹ Voevodsky Institute of Chemical Kinetics and Combustion SB RAS, Novosibirsk, Russia

² Departamento de Química/Instituto de Tecnología Química UPV-CSIC, Valencia, Spain

*Address all correspondence to: khramtsovaea@gmail.com

IntechOpen

© 2018 The Author(s). Licensee IntechOpen. This chapter is distributed under the terms of the Creative Commons Attribution License (<http://creativecommons.org/licenses/by/3.0>), which permits unrestricted use, distribution, and reproduction in any medium, provided the original work is properly cited. 

References

- [1] Lin GQ, You QD, Cheng JF. *Chiral Drugs: Chemistry and Biological Action*. Hoboken: Wiley; 2011
- [2] Jiménez MC, Pischel U, Miranda MA. Photoinduced processes in naproxen-based chiral dyads. *Journal of Photochemistry and Photobiology C: Photochemistry Reviews*. 2007;**8**:128-142. DOI: 10.1016/j.jphotochemrev.2007.10.001
- [3] Khramtsova EA, Sosnovsky DV, Ageeva AA, Nuin E, Marin ML, Purtov PA, et al. Impact of chirality on the photoinduced charge transfer in linked systems containing naproxen enantiomers. *Physical Chemistry Chemical Physics*. 2016;**18**: 12733-12741. DOI: 10.1039/C5CP07305G
- [4] Duggan KC, Hermanson DJ, Musee J, Prusakiewicz JJ, Scheib JL, Carter BD, et al. (R)-Profens are substrate-selective inhibitors of endocannabinoid oxygenation by COX-2. *Nature Chemical Biology*. 2011;**7**:803-809. DOI: 10.1038/NChemBio.663
- [5] Bonancia P, Vaya I, Climent MJ, Gustavsson T, Markovitsi D, Jiménez MC, et al. Excited-state interactions in diastereomeric flurbiprofen-thymine dyads. *Journal of Physical Chemistry A*. 2012;**116**:8807-8814. DOI: 10.1021/jp3063838
- [6] Vaya I, Jiménez MC, Miranda MA. Excited-state interactions in flurbiprofen-tryptophan dyads. *Journal of Physical Chemistry B*. 2007;**111**:9363-9371. DOI: 10.1021/jp071301z
- [7] Vaya I, Gustavsson T, Markovitsi D, Miranda MA, Jiménez MC. Influence of the spacer on the photoreactivity of flurbiprofen-tyrosine dyads. *Journal of Photochemistry and Photobiology A: Chemistry*. 2016;**322-323**:95-101. DOI: 10.1016/j.jphotochem.2016.03.006
- [8] Limones-Herrero D, Pérez-Ruiz R, Lence E, González-Bello C, Miranda MA, Jiménez MC. Mapping a protein recognition centre with chiral photoactive ligands. An integrated approach combining photophysics, reactivity, proteomics and molecular dynamics simulation studies. *Chemical Science*. 2017;**8**:2621-2628. DOI: 10.1039/C6SC04900A
- [9] Lhiaubet-Vallet V, Bosca F, Miranda MA. Stereodifferentiating drug biomolecule interactions in the triplet excited state: Studies on supramolecular carprofen/protein systems and on carprofen-tryptophan model dyads. *Journal of Physical Chemistry B*. 2007;**111**:423-431. DOI: 10.1021/jp066968k
- [10] Vaya I, Jiménez MC, Miranda MA, Chatterjee A, Gustavsson T. Ultrafast fluorescence dynamics in flurbiprofen-amino acid dyads and in the supramolecular drug/protein complex. *Chimia*. 2017;**71**:18-25. DOI: 10.2533/chimia.2017.18
- [11] Magin IM, Polyakov NE, Khramtsova EA, Kruppa AI, Tsentalovich YP, Leshina TV, et al. Spin effects in intramolecular electron transfer in naproxen-N-methylpyrrolidine dyad. *Chemical Physics Letters*. 2011;**516**:51-55. DOI: 10.1016/j.cplett.2011.09.057
- [12] Magin IM, Polyakov NE, Khramtsova EA, Kruppa AI, Stepanov AA, Purtov PA, et al. Spin chemistry investigation of peculiarities of photoinduced electron transfer in donor-acceptor linked system. *Applied Magnetic Resonance*. 2011;**41**:205-220. DOI: 10.1007/s00723-011-0288-3
- [13] Khramtsova EA, Plyusnin VF, Magin IM, Kruppa AI, Polyakov NE, Leshina TV, et al. Time-resolved fluorescence study of exciplex formation in diastereomeric naproxen-pyrrolidine

dyads. *Journal of Physical Chemistry B*. 2013;**117**:16206-16211. DOI: 10.1021/jp4083147

[14] Khramtsova EA, Ageeva AA, Stepanov AA, Plyusnin VF, Leshina TV. Photoinduced electron transfer in dyads with (R)-/(S)-naproxen and (S)-tryptophan. *Zeitschrift für Physikalische Chemie*. 2017;**231**: 609-623. DOI: 10.1515/zpch-2016-0842

[15] Ageeva AA, Khramtsova EA, Magin IM, Rychkov DA, Purtov PA, Miranda MA, et al. Spin selectivity in chiral linked systems. *Chemistry—A European Journal*. 2018;**24**:3882-3892. DOI: 10.1002/chem.201705863

[16] Weller AZ. Photoinduced electron transfer in solution: Exciplex and radical ion pair formation free enthalpies and their solvent dependence. *Zeitschrift für Physikalische Chemie*. 1982;**133**:93-98. DOI: 10.1524/zpch.1982.133.1.093

[17] Perez-Ruiz R, Gil S, Miranda MA. Stereodifferentiation in the photochemical cycloreversion of diastereomeric methoxynaphthalene-oxetane dyads. *Journal of Organic Chemistry*. 2005;**70**:1376-1381. DOI: 10.1021/jo048708

[18] Salikhov KM, YuN M, Sagdeev RZ, Buchachenko AL. *Spin Polarization and Magnetic Effects in Radical Reactions*. Budapest, Hungary: Akademiai Kiado; 1984. pp. 65-72

[19] Pischel U, Abad S, Miranda MA. Stereoselective fluorescence quenching by photoinduced electron transfer in naphthalene-amine dyads. *Chemical Communications*. 2003;**9**: 1088-1089. DOI: 10.1039/b301414b

[20] Magin IM, Polyakov NE, Kruppa AI, Purtov PA, Leshina TV, Kiryutin AS, et al. Low field photo-CIDNP in the intramolecular electron transfer of naproxen-pyrrolidine dyads. *Physical Chemistry Chemical Physics*. 2016;**18**:901-907. DOI: 10.1039/c5cp04233j

[21] Kreilick RW, Becher J, Ullman EF. Electron spin resonance studies of nitronylnitroxide radicals with asymmetric centers. *Journal of the American Chemical Society*. 1969;**91**:5121-5124. DOI: 10.1021/ja01046a032

[22] Levkin A, Kolb HJ, Kokorin AI, Schurig V, Kostyanovsky RG. Solid-state ESR differentiation between racemate versus enantiomer. *Chirality*. 2006;**18**:232-238. DOI: 10.1002/chir.20242

[23] Maeurer M, Stegmann HB. Chiral recognition of diastereomeric esters and acetals by EPR and NMR investigations. *Chemische Berichte*. 1990;**123**: 1679-1685. DOI: 10.1002/cber.19901230817

[24] Aladekomo JB, Birks JB. 'Excimer' fluorescence. VII. Spectral studies of naphthalene and its derivatives. *Proceedings of the Royal Society of London A*. 1965;**284**:551-565. DOI: 10.1098/rspa.1965.0080

[25] Jimenez MC, Pischel U, Miranda MA. Photoinduced processes in naproxen-based chiral dyads. *Journal of Physical Chemistry C*. 2007;**8**:128-142. DOI: 10.1016/j.jphotochemrev.2007.10.001

[26] Pracz M, Franska M, Franski R. Mass spectrometric study of naproxen dimer anions generated from racemate and pure enantiomers. *Journal of Chemical and Pharmaceutical Research*. 2012;**4**:231-238

[27] Naaman R, Waldeck D. Chiral-induced spin selectivity effect. *Journal of Physical Chemistry Letters*. 2012;**3**:2178-2187. DOI: 10.1021/jz300793y

[28] Frank FC. On spontaneous asymmetric synthesis. *Biochimica et Biophysica Acta*. 1953;**11**:459-463. DOI: 10.1016/0006-3002(53)90082-1